COBEM 2023 27TH INTERNATIONAL CONGRESS OF MECHANICAL ENGINEERING

ABCM Brazilian Society of Mechanical Sciences and Engineering
27th ABCM International Congress of Mechanical Engineering
December 04-08, 2023, Florianópolis-SC, Brazil

COB-2023-2409
TRANSIENT FLOWS WITH CAVITATION OF BIODIESEL IN PIPELINES

Elias do Carmo Dias
Helcio Rangel Barreto Orlande
Federal University of Rio de Janeiro – UFRJ/COPPE, Rio de Janeiro, RJ, Brazil
elias.cd@mecanica.coppe.ufrj.br, hrborlande@gmail.com

Marcelo José Colaço
Federal Univesity of Rio de Janeiro – UFRJ/COPPE, Rio de Janeiro, RJ, Brazil
mc@pobox.com

Ítalo Marcio Madeira
Cenpes – Petrobras's Research, Development and Inovation Center, Rio de Janeiro, RJ, Brazil
italomadeira@petrobras.com.br

Abstract. *Transient flows with cavitation are of great importance in transport of fuels through pipelines. Fossil fuels may cause several problems to the environment, such as air pollution and emissions of greenhouse gases, which contribute to global warming. Biofuels are a viable alternative to partially replace fossil fuels. This work aims at the implementation of a computer code for the simulation of transient flows of biofuels in pipelines during cavitation. The model used was one-dimensional and involved a homogeneous mixture. The numerical solution was obtained with the finite volumes method, where the FLIC (Flux Limited Centered) and the WAF-TVD (Weighted Average Flux – Total Variation Diminishing) numerical schemes were compared for the solution of the resulting homogeneous system of partial differential equations. In addition, the Euler, Runge-Kutta and Bulirsch-Stoer methods were compared for the solution of the non-homogeneous system of ordinary equations. The obtained results revealed that the FLIC scheme combined with the Bulirsch-Stoer method, resulted in solutions with smaller oscillations originated from cavitation. Our solution was verified by using literature data and validated with experiments using water in an actual pipeline. After verification and validation, simulations were performed with biodiesel, which revealed that pressure peaks during cavitation were higher for water than for biodiesel under similar conditions.*

Keywords: *Cavitation, finite volumes, biofuels, transient flows*

1. INTRODUCTION

The comprehension of transient flows in pipelines is very important for engineering applications. There is a great interest in developing models that are capable of simulating this phenomenon. In a pipeline, when the velocity of the flow sudden changes, a pressure pulse is created, moving with the velocity of sound. This phenomenon is called water hammer and its main causes are pump starting and stopping, pipe rupture and valve opening and closing maneuvers (Jensen et al., 2018). During the hydraulic transient, when the pressure reaches the vapor pressure of liquid, the one-phase flow (liquid) changes to two-phase flow (liquid and vapor) through the bubbles in the liquid. This phenomenon is called vapor cavitation (Bergant et al., 2006). The raise and collapse of bubbles can lead to higher pressure peaks than water hammer and can cause several problems such as flow rate fluctuation, load asymmetry, vibrations and noise (Sumam et al., 2009). In order to avoid these problems, there is a motivation in developing models that can predict and describe vapor cavitation.

In this work a model is applied to analyze cavitation in water and biodiesel flows. The main hypothesis is that when cavitation happens we have a homogeneous mixture with bubbles uniformly distributed through the liquid. The mathematical model is based on the conservation of mass and momentum, and a transport equation for the void fraction. The dependent variables to be evaluated are density, velocity and vapor mass fraction. To compute the pressure, a constitutive relationship is presented. The numerical solutions were obtained via the finite volumes method. The differential system of equations was solved using two steps. First, a homogeneous system of partial equations was solved and then a non-homogeneous system of ordinary equations was evaluated. Since the equations are complicated, several numerical methods were compared to obtain the best solution methods for the problem. For the homogeneous system of partial differential equations, the FLIC and the WAF-TVD numerical schemes were compared and for the non-homogeneous system of ordinary equations the Euler, Runge-Kutta and Bulirsch-Stoer methods were studied. The constitutive equation to evaluate the pressure could not be solved analytically, and for this reason the Newton-Raphson method was used to solve it. The computational implementation of the model was made in C++.

Most works in the literature simulated cavitation only in the presence of water, such as Sumam et al. (2009), Sadafi et al. (2012), Soares et al. (2015), Zhou et al. (2017) and Sun et al. (2020). This work used water to make the verification

and validation and then used the model to compare cavitation in the presence of water and biodiesel. This biofuel was chosen since it plays a huge role in the industry being a good alternative to partially replace fossil fuels.

2. MATHEMATICAL MODEL

The fluid-flow problem analyzed in this work is one dimensional, in a pipeline with a diameter *D*. The pipeline changes its elevation and local losses were also considered. The hydraulic transient is caused by opening and closing a valve in the end of the pipe. The hypotheses applied to the model were the same studied by Sumam et al. (2009): the flow is one dimensional; the vapor bubbles are small, spherical in shape and uniformly distributed; the difference in pressure across a bubble due to surface tension can be neglected and the two phases have the same velocity which allows the assumption of homogeneous mixture.

The one dimensional continuity equation for homogeneous mixture is given by (Wilie and Streeter, 1978)

$$\frac{\partial \rho}{\partial t} + \frac{\partial (\rho u)}{\partial x} = 0, \tag{1}$$

where *x*, *t*, ρ and *u* are the pipe coordinate in the direction of the flow, time, density and velocity of the flow respectively.

The one dimensional momentum equation for the homogeneous mixture including local losses and acceleration losses can be written as (Wilie and Streeter, 1978), (Michaelides et al., 2016) and (Carvalho, 2020)

$$\frac{\partial (\rho u)}{\partial t} + \frac{\partial (p+\rho u^2)}{\partial x} + \rho g sen\theta + \frac{f \rho u |u|}{2D} + (\rho u)^2 \frac{\partial \vartheta}{\partial x} + k_l \frac{\rho u^2}{2} \delta(x - x_l) = 0, \tag{2}$$

where *p*, *g*, θ, *f* and *D* are the absolute pressure, gravitational acceleration, elevation angle, friction factor and cross sectional diameter respectively. The parameter ϑ is the specific volume of the mixture; k_l and x_l are the coefficient and the position relative to local losses respectively; and δ is the Dirac delta function.

To compute the mass transfer between the phases we used a transport equation for the volume void fraction which is given by (Singhal et al., 2002)

$$\frac{\partial (\rho_v \alpha_v)}{\partial t} + \frac{\partial (\rho_v \alpha_v u)}{\partial x} = R_e - R_c, \tag{3}$$

where ρ_v, α_v, R_e and R_c are the vapor density, volume void fraction, vapor generation (evaporation) and vapor collapse (condensation) respectively.

Equations. (1), (2) and (3) can be written in the matrix form as:

$$\frac{\partial \mathbf{U}}{\partial t} + \frac{\partial \mathbf{F(U)}}{\partial x} = \mathbf{S(U)}, \tag{4}$$

where **U**, **F(U)** and **S(U)** are the state vector, flux vector and the source term vector respectively, given by:

$$\mathbf{U} = \begin{pmatrix} \rho \\ \rho u \\ \rho_v \alpha_v \end{pmatrix}, \tag{5}$$

$$\mathbf{F(U)} = \begin{pmatrix} \rho u \\ p + \rho u^2 \\ \rho_v \alpha_v u \end{pmatrix}, \tag{6}$$

and

$$\mathbf{S(U)} = \begin{pmatrix} 0 \\ -\rho g sen\theta - \frac{f \rho u |u|}{2D} - (\rho u)^2 \frac{\partial \vartheta}{\partial x} - k_l \frac{\rho u^2}{2} \delta(x - x_l) \\ R_e - R_c \end{pmatrix}. \tag{6}$$

Singhal et al. (2002) presented an equation to calculate the terms R_e and R_c, given by Eqs. (7) and (8).

$$R_e = C_e \frac{\sqrt{k}}{\sigma} \rho_l \rho_v \left[\frac{2}{3} \frac{p_v - p}{\rho_l} \right]^{1/2} \left(1 - \frac{\rho_v \alpha_v}{\rho} \right) \tag{7}$$

$$R_c = C_c \frac{\sqrt{k}}{\sigma} \rho_l \rho_l \left[\frac{2}{3} \frac{p - p_v}{\rho_l} \right]^{1/2} \left(\frac{\rho_v \alpha_v}{\rho} \right) \tag{8}$$

where σ is the surface tension and k is turbulent kinetic energy, given by $\sqrt{k} = 0.1u$. C_e and C_c are empirical constants related to evaporation and condensation respectively and their recommended values are 0.02 and 0.01 (Singhal et al., 2002). ρ_l and p_v are the liquid density and vapor pressure respectively.

To compute the pressure a constitutive relationship is needed. Sumam et al., (2009) presented the relation between the variables of the state vector and the pressure showed in Eq. (9)

$$\rho_{l_0} e^{\frac{(p-p_0)}{k_l}} \left(1 - \frac{\rho_v \alpha_v RT}{pM}\right) + \rho_v \alpha_v - \rho = 0, \tag{9}$$

where ρ_{l_0}, p_0, k_l, R, M and T are the density at standard conditions, pressure at standard conditions, bulk modulus of liquid, gas constant, molar mass and temperature.

3. SOLUTION METHODS

Toro (2009) and OZISIK et al. (2017) established that a system of partial differential equations with a source term can be split in a homogeneous system of partial equations and a non-homogeneous system of ordinary equations. The system in Eq. (4) can be written as (Toro, 2009) and (OZISIK et al., 2017)

$$\left.\begin{array}{l} \frac{\partial \mathbf{U}}{\partial t} + \frac{\partial \mathbf{F(U)}}{\partial x} = 0 \\ \mathbf{U} = \mathbf{U}^{\mathrm{n}} \end{array}\right\} = \bar{\mathbf{U}}^{\mathrm{n+1}}, \tag{10}$$

and

$$\left.\begin{array}{l} \frac{\partial \mathbf{U}}{dt} = \mathbf{S(U)} \\ \mathbf{U} = \bar{\mathbf{U}}^{\mathrm{n+1}} \end{array}\right\} = \mathbf{U}^{\mathrm{n+1}}, \tag{11}$$

where the solution of the system (10) is the initial condition of system (11).

3.1 Methods for the homogeneous system of differential partial equations

The finite volume method was used in this work. The system of equations (10) can be integrated and solved using a conservative scheme given by (Toro, 2009)

$$\mathbf{U}_{\mathrm{i}}^{\mathrm{n+1}} = \mathbf{U}_{\mathrm{i}}^{\mathrm{n}} + \frac{\Delta \mathrm{t}}{\Delta \mathrm{x}} \left(\mathbf{F}_{\mathrm{i-1/2}}^{\mathrm{n}} - \mathbf{F}_{\mathrm{i+1/2}}^{\mathrm{n}}\right) \tag{12}$$

where Δt, Δx and $\mathbf{F}^{\mathrm{n}}$ are the time step, volume size and the flux between two adjacent volumes respectively.

To evaluate the flux two schemes were applied, FLIC and WAF-TVD. The FLIC scheme combines a low order monotone flux with a high order flux. Being a TVD scheme, it gives stability to the solution. The equation to calculate the flux is given by (Toro, 2009)

$$\mathbf{F}_{\mathrm{i+1/2}} = \mathbf{F}_{\mathrm{i+1/2}}^{\boldsymbol{LO}} + \emptyset_{\mathrm{i+1/2}} \left[\mathbf{F}_{\mathrm{i+1/2}}^{\boldsymbol{HO}} - \mathbf{F}_{\mathrm{i+1/2}}^{\boldsymbol{LO}}\right] \tag{13}$$

where $\mathbf{F}_{\mathrm{i+1/2}}^{\boldsymbol{LO}}$, $\mathbf{F}_{\mathrm{i+1/2}}^{\boldsymbol{HO}}$ and $\emptyset_{\mathrm{i+1/2}}$ are the low order flux, high order flux and the limiter function respectively. Toro (2009) established for this approach that the low order flux is given by the FORCE flux and the high order flux is given by the Richtmyer flux. The limiter function used is this work is the VANLEER function described in Toro (2009). The FORCE flux is defined as a mean of Lax Friedrichs and Richtmyer fluxes (Toro, 2009).

The WAF-TVD scheme is a generalization of first order upwind schemes (Toro, 2009). The equation to evaluate the flux between two volumes is given by (Toro, 2009)

$$\mathbf{F}_{\mathrm{i+1/2}} = \frac{\mathbf{1}}{\mathbf{2}} (\mathbf{F}_{\mathrm{i}} + \mathbf{F}_{\mathrm{i+1}}) - \frac{\mathbf{1}}{\mathbf{2}} sign(c_k) \emptyset_{\mathrm{i+1/2}}^{(k)} \Delta \mathbf{F}_{\mathrm{i+1/2}}^{(\boldsymbol{k})} \tag{14}$$

where $sign(c_k)$ is the sign function and the parameter c_k is related to the wave velocity. The term $\Delta \mathbf{F}_{\mathrm{i+1/2}}^{(\boldsymbol{k})}$ in Eq. (14) is the jump across wave k (Toro, 2009).

3.2 Methods for the non-homogeneous system of ordinary equations

The system of ordinary equations for this problem represents a stiff problem according to the conditions established by Toro (2009). A stiff problem can lead to oscillations in the solution. Three explicit methods were studied to obtain the solution of the system (11): the Euler method, the Runge-Kutta method and the Bulirsch Stoer method. The equation for the Euler method is given by (Toro, 2009)

$$\mathbf{U}_{\mathrm{i}}^{\mathrm{n+1}} = \mathbf{U}_{\mathrm{i}}^{\mathrm{n}} + \Delta \mathrm{t}\mathbf{S}(t^n, \bar{\mathbf{U}}^{\mathrm{n+1}}) \tag{15}$$

The fourth order Runge-Kutta method is more complex and it is solved in five steps according to the equations below (Toro, 2009).

$$\begin{cases} \mathbf{K}_1 = \Delta \mathrm{t}\mathbf{S}(t^n, \mathbf{U}^{\mathrm{n}}) \\ \mathbf{K}_2 = \Delta \mathrm{t}\mathbf{S}\left(t^n + \frac{1}{2}\Delta \mathrm{t}, \mathbf{U}^{\mathrm{n}} + \frac{1}{2}\mathbf{K}_1\right) \\ \mathbf{K}_3 = \Delta \mathrm{t}\mathbf{S}\left(t^n + \frac{1}{2}\Delta \mathrm{t}, \mathbf{U}^{\mathrm{n}} + \frac{1}{2}\mathbf{K}_2\right) \\ \mathbf{K}_4 = \Delta \mathrm{t}\mathbf{S}(t^n + \Delta \mathrm{t}, \mathbf{U}^{\mathrm{n}} + \mathbf{K}_3) \\ \mathbf{U}^{\mathrm{n+1}} = \mathbf{U}^{\mathrm{n}} + \frac{1}{6}[\mathbf{K}_1 + 2\mathbf{K}_2 + 2\mathbf{K}_3 + \mathbf{K}_4] \end{cases}, \tag{16}$$

The Bulirsch-Stoer method is based on the modified middle point method and the Richardson extrapolation (Ribeiro et al., 2022). The advantage of this method is that it splits the time step in smaller intervals to control the error (Bulirsch and Stoer, 1992). To implement this method a Odeint library was used (Ahnert and Mulansky, 2011).

3.3 Newton Raphson method

Equation (9) was used to calculate the pressure. This equation cannot be solved analytically, being necessary a numerical method to solve it. Eq. (9) can be rewritten as

$$f(p) = \rho_{l_0} e^{\frac{(p-p_0)}{k_l}} \left(1 - \frac{\rho_v \alpha_v RT}{pM}\right) + \rho_v \alpha_v - \rho = 0, \tag{17}$$

which is differentiable in p. Then the Newton-Raphson method was used in the form (Hildebrand, 1974)

$$p^{q+1} = p^q - \frac{f(p^q)}{f'(p^q)}, \tag{18}$$

where q is the iteration number. Equation (18) is used until the pressure value converge.

4. RESULTS

4.1 Verification

The verification of the code was made in two parts. In the first part we reproduced results from literature where the simulation was made in a simple straight pipeline. In the second part we performed simulations in a complex pipeline with elevations. The purpose of the second part was to compare the solution methods for the system of ordinary equations described in section 3.2.

The first stage of the verification was a comparison with the results obtained by Sumam et al. (2009). Sumam performed experiments using water in a straight pipeline made of steel. The length of the pipeline was 32.5m and the volumetric flow rate was 0.000562 m^3/s . The transient regime was generated by a sudden valve closure at the end of the pipeline. The analyzed results are the pressure variations in the valve section along the time. The total time of the experiment was 0.5s and the time of valve closure varied from 0 to 0.02s. Figure 1 shows the pressure at the valve position for Sumam et al. (2009) results. Figure 2 shows the pressure at the valve position calculated with the model presented here. For the homogeneous system presented in Eq. (10), FLIC and WAF-TVD schemes were compared. Since it is a very simple pipeline for the non-homogeneous system presented in Eq. (11) only the Euler method was used.

The pressure rise started at the 0.167 MPa which is the initial value. Due the valve closure, the pressure rises up to 0.5MPa and then falls to a value below the vapor pressure when the evaporation starts. When the pressure rises again, the vapor collapse occurs, and we have a higher pressure peak. The cycle of evaporation and condensation continues but the wave loses energy because of the friction.

The results showed that the model presented here with both solutions methods produced very close results to the literature data. The WAF-TVD showed some artificial peaks while FLIC scheme was very stable. Since FLIC produced better results and less computational time it was used for the next sections.

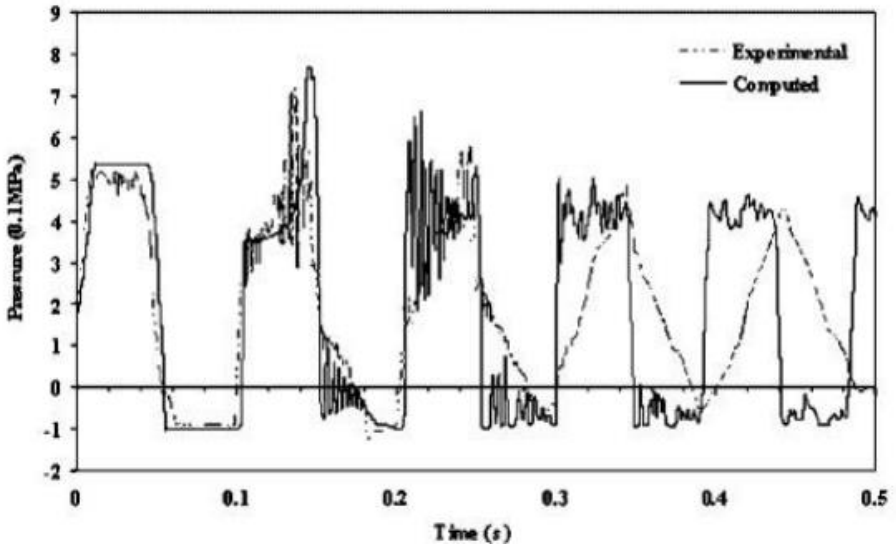

Figure 1. Results presented in Sumam et al. (2009).

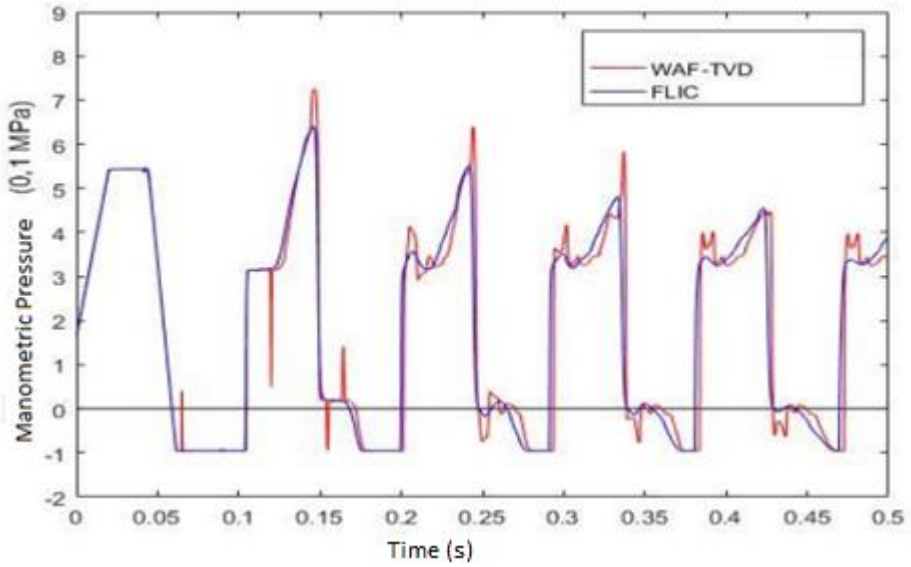

Figure 2. Results with FLIC and WAF-TVD schemes.

The second part of the verification step was made considering a steady state flow in the actual pipeline where the experiments were planned. This pipeline is located in the Technological Center of Ducts (CTDUT) and it has a complex geometry with several local losses. The total length is 2473m with a diameter of 0.3m. Figure 3 shows the pipe profile, where we can see a region with a maximum elevation called shelter.

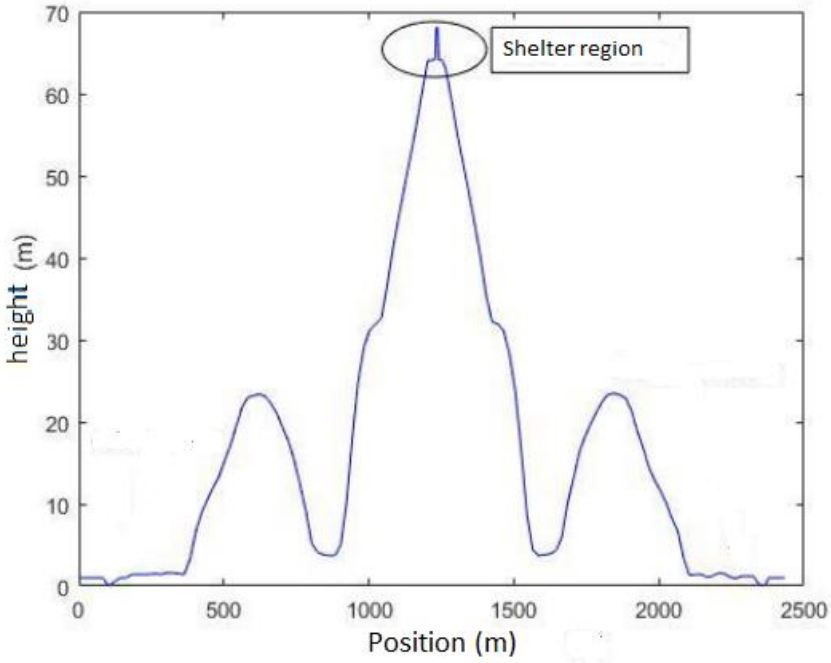

Figure 3. CTDUT Pipeline profile.

The boundary conditions for this simulation were the pressure at end walls of the pipeline. The calculated volumetric flow rate was used as a result. The pressure values were chosen to have cavitation due the elevation in the shelter region. The values were $7.74 kgf/cm^2$ at the beginning and $5.50 kgf/cm^2$ at the end of the pipe. Cavitation produced oscillations in the final results and that is why a good method to integrate the ordinary system is needed. Figure 4 shows the volumetric flow rate at the end of the pipeline using the methods described in section 3.2. We can see that up to 50 seconds there are big oscillations which correspond to the adjustment of the initial condition. After 50 seconds the oscillations are smaller and we can see the difference between the methods. The Bulirsch-Stoer method reduced considerably the oscillations in comparison to the other methods showing better results for this complex pipeline.

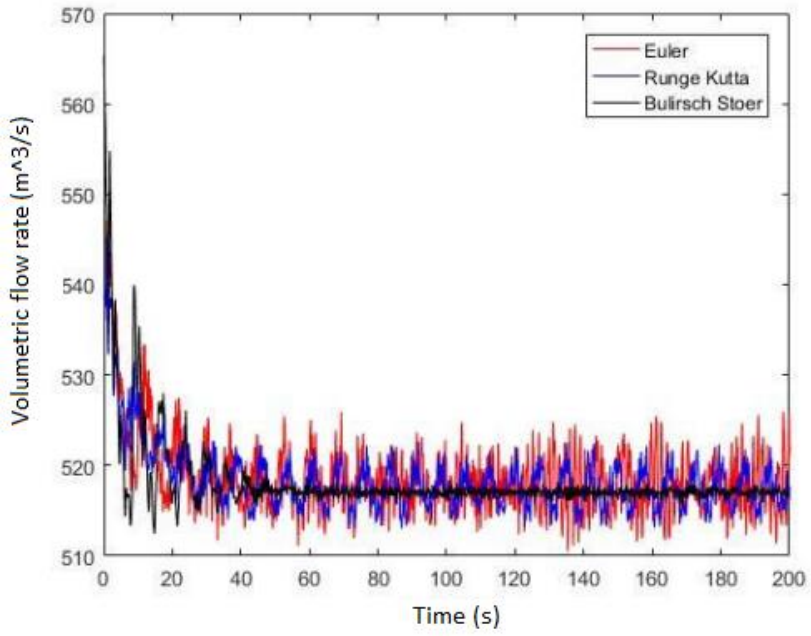

Figure 4. Comparison between Euler, Runge Kutta and Bulirsch-Stoer methods.

4.2 Validation

To validate the model an experiment was performed in Technological Center of Ducts in the pipeline showed in figure 3. The experiment lasted for 1400 seconds and the sensors monitored the pressure and volumetric flow rate in two positions, upstream and downstream. The fluid used was water and it started in a steady state regime without cavitation. Figure 5 shows the pressure and volumetric flow rate measurements throughout the experiment. The experiment starts in steady state as we can see a constant pressure profile up to 270 seconds. After this, a valve at the end of the pipeline is partially open and then partially closed generating a transient regime from 270 to 370 seconds approximately. A second steady regime state is observed from 380 to 470 seconds approximately. After this second steady state regime, a new transient happens from 570 to 700 seconds. After 700 seconds the final steady state is established.

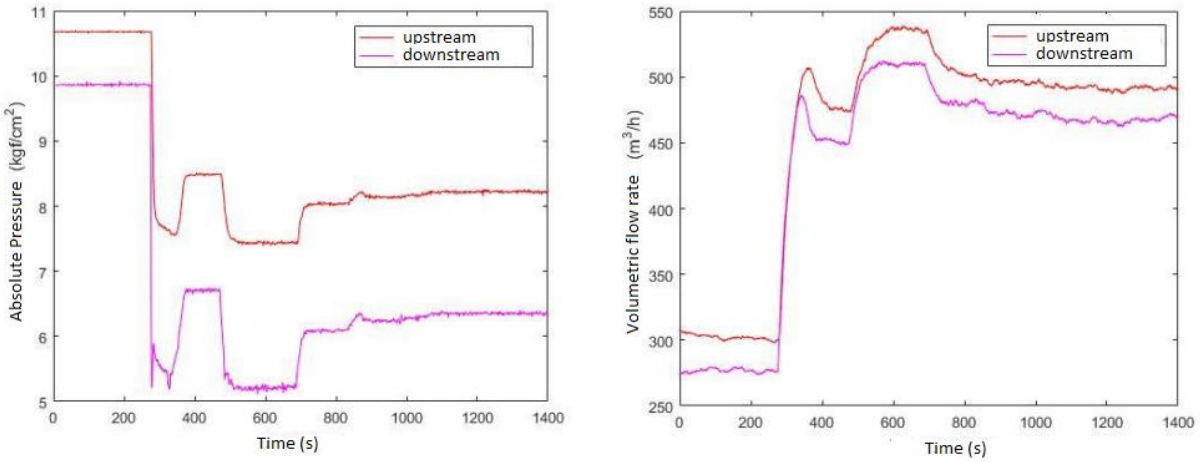

Figure 5. Pressure and volumetric flow rate measurements of the real experiment

Figure 6 shows a comparison of the volumetric flow rate, measured and calculated with the model. The figure also shows the error bars using confidence interval of 99% of the measurement. We can see that the calculated value upstream and downstream are close to the data obtained from the sensors, which means that the model can simulate the experiment successfully. The right side of Figure 6 presents the volume void fraction in the upstream, downstream and shelter region throughout the experiment to track the cavitation. It can be observed that cavitation only happens at shelter region during the transient time. At the beginning and end of the pipe void fraction remain close to zero with the maximum value close to $1x10^{-7}$. At the shelter region it reaches the maximum value of approximately 0.065, which means a considerable amount of vapor. This section showed that the model can simulate cavitation successfully with a stable solution, even for a complex pipeline with elevations and local losses.

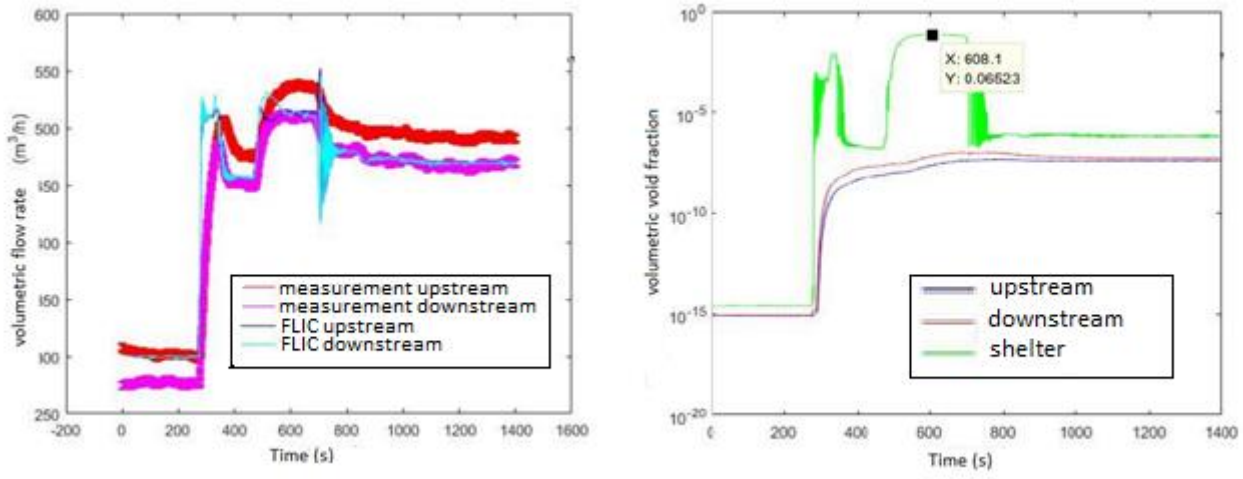

Figure 6. Comparison between experimental and simulated results

4.3 Simulation with biodiesel

Most works in the literature that approach cavitation study the phenomenon only in the presence of water. In this work we analyzed cavitation also in the presence of biodiesel. Since the model was validated with water in the last section we can apply it to the other fluids once their physical properties are available. The biodiesel studied here was the soy kind and its properties were obtained from the literature. Vargas et al. (2017) gave the density and the kinematic viscosity in their work. The bulk modulus was obtained in Rocha (2019) and the surface tension was given by Prado and Morita (2015). Pulido et al. (2019) presented the vapor pressure of biodiesel used in his work. The Table 1 shows the comparison of the main properties to water and soy biodiesel.

Table 1. Water and biodiesel properties

Properties	**Water**	**Biodiesel**
Density, kg/m^3	1000	875
Kinematic viscosity, m^2s^{-1}	9.84×10^{-7}	6.0×10^{-6}
Bulk modulus, GPa	2.15	1.04
Surface tension, N/m	0.072	0.031
Vapor pressure, Pa	2330	670

The numerical simulation to compare water and biodiesel during cavitation was made in the CTDUT pipeline, which was used for validation. The simulation starts in steady state with pure liquid and then a transient was originated by a valve closure at the end of the pipeline. The valve closure lasted for one second which led to the cavitation phenomenon at the valve position. Figure 7 shows the pressure at the valve position for 20 seconds after the valve closure. We can see that pressure falls below the vapor pressure generating bubbles which lead to cavitation. The pressure peaks are higher for water than biodiesel and the wave frequency is also higher for water. Figure 8 shows the void fraction during the phenomenon where we can see that this parameter grows when the pressure stays below the vapor pressure. The void fraction was higher to water than biodiesel meaning a bigger amount of vapor.

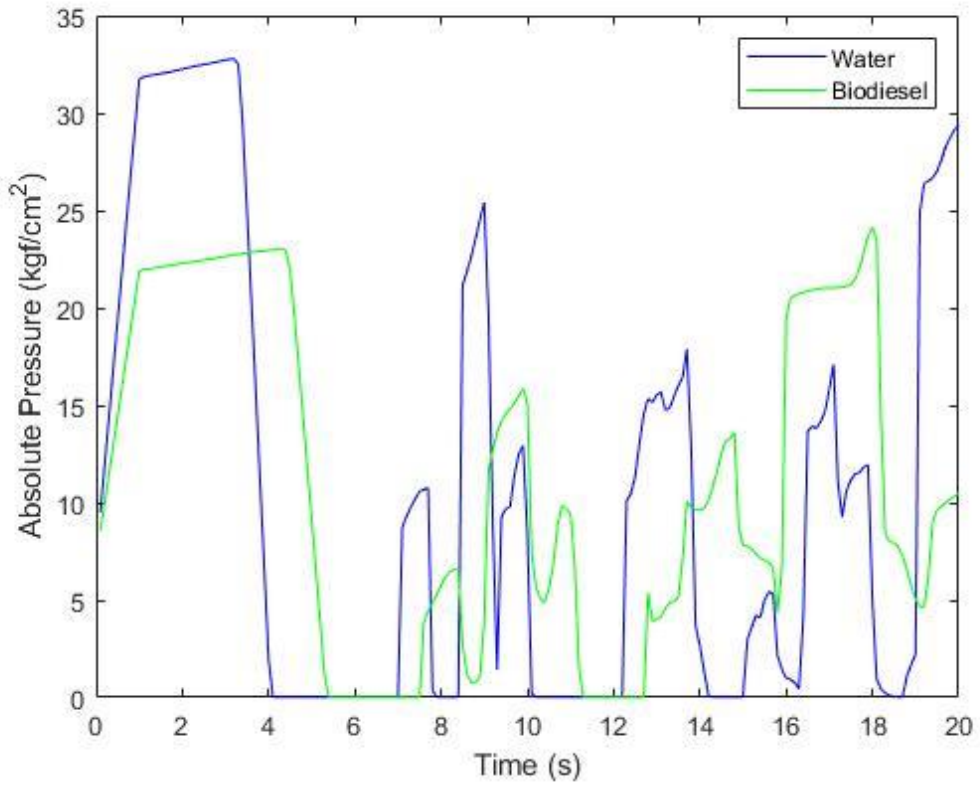

Figure 7. Pressure of water and biodiesel during cavitation

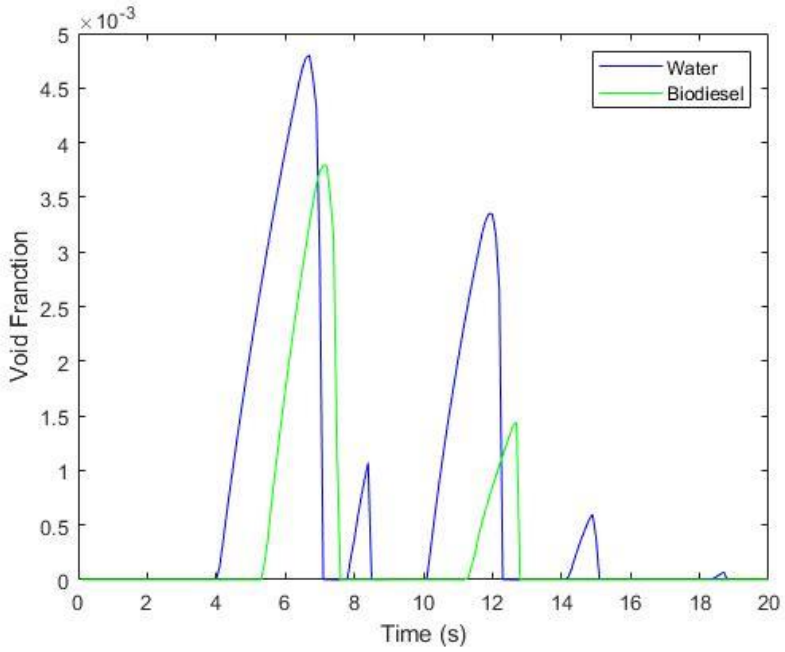

Figure 8. Void fraction of water and biodiesel during cavitation

5. CONCLUSIONS

This work presented a solution model to simulate cavitation. The model was based on the conservation of mass, and momentum and a transport equation for the void fraction. To compute the pressure, a constitutive relationship was presented. Several solution methods were studied. The model was validated and then used to perform simulations using water and biodiesel. The main conclusions of the study are:

• The model presented in this work can simulate cavitation successfully since it was verified with literature results and validated with experiments.

• In the pipeline without elevations the Euler method presented good results solving the non-homogeneous system of ordinary equations. For this pipeline FLIC and WAF-TVD method were used to solve the homogeneous system of partial equations. Both methods presented good results however WAF-TVD method presented artificial pressure peaks while FLIC provided a more stable solution.

• In the complex pipeline with elevations and local losses the Euler and Runge-Kutta methods presented oscillations while Bulirsch-Stoer method could provide stable results reducing considerably the oscillations caused by the cavitation phenomenon.

• Simulations were performed for transient flow with cavitation using water and biodiesel in similar conditions. The results showed that cavitation is more severe for water leading to a higher pressure peaks and a bigger amount of vapor.

6. ACKNOWLEDGEMENTS

This paper was partially funded by the following Brazilian agencies: CNPq (Brazilian National Council for Scientific and Technological Development), FAPERJ (Rio de Janeiro State Agency for Research) and ANP-PRH8 (Brazilian National Regulatory Agency for Oil, Gas and Biofuels – Human Research Program number 8).

We thank to the Technological Center of Ducts (CTDUT) for the support in the experiments to validate the model.

7. REFERENCES

BERGANT, A., SIMPSON, A. R., TIJSSELING, A. S., 2006, Water Hammer with Column Separation: A Historical Review, Journal of Fluids and Structures, v. 22 (2), pp. 135-171.

CARVALHO, R. C., 2018, Estudo Numérico do Problema do Golpe de Aríete em Tubulações. Projeto Final de Graduação, DEM/UFRJ, Rio de Janeiro, RJ, Brasil.

HILDEBRAND, F. B., 1974, Introduction to Numerical Analysis. 2 ed. New York.

JENSEN, R. K., LARSEN, J. K., LASSEN, K. L., MANDO, M., ANDREASEN, A., 2018, Implementation and Validation of a Free Open Source 1D Water Hammer Code, Journal of Fluids, pp. 3-64.

MICHAELIDES. E. E., CROWE T. C., SCHWARZKOPF, D. JOHN., 2016, Multiphase Flow Handbook, 2 ed., CRC Press.

MULANSKY, M., AHNERT, K., 2011, "Odeint – Solving Ordinary differential equations in C++", AIP Conf. Numerical Analysis Applied Mathematics, v. 1389, pp. 1586-158

OZISIK, N., ORLANDE, H. R. B., COLAÇO, M. J., COTTA, R. M., 2017, Finite Difference Methods in Heat Transfer. 2 ed., CRC Press.

PRADO, M. V. B., MORITA, D. M., 2013, "Influência do Biodiesel de Origem Vegetal na Tensão Superficial e Interfacial do Diesel", III Congresso Internacional de Meio Subterrâneo

PULIDO, J. L., MORENO, W. S. F., TAPIA, M. J. A., DELGADO, A. D. G., CONCHA, V. O. C., NUNHEZ, J. R., 2019, "Estudo termoquímico assistido por computador para a produção de biodiesel", Revista Ion, v. 32, n.2, pp 2145-2153.

ROCHA, A. S., 2019, Previsão das Propriedades Termodinâmicas do Biodiesel e Diesel Comum, Suas Blendas e Efeitos de Aditivos Via Teoria do Funcional da Densidade e Ensemble Canônico. Tese de Doutorado, ITEC/UFPA, Belém, PA, Brasil.

SADAFI, M., RIASI, A., NOURBAKHSH, S. A., 2012, "Cavitating Flow During Water Hammer Using a Generalized Interface Vaporous Cavitation Model", Journal of Fluids and Structures, v. 34, pp. 190-201.

SINGHAL, A. K., ATHAVALE, M. M., LI, H., JIANG, Y., 2002, "Mathematical Basis and Validation of Full Cavitation Model", Journal of Fluids Engineering, v. 124, pp. 617- 624

SOARES, A. K., MARTINS, N., COVAS, D. I. C., 2015," Investigation of Transient Vaporous Cavitation: Experimental and Numerical Analyses", Procedia Engineering 119, pp. 235-242.

SUMAM, K. S., THAMPI, S. G., SAJIKUMAR, N., 2009, "An Alternative Approach for Modeling of Transient Vaporous Cavitation", International Journal for Numerical Methods in Fluids, v. 63, pp. 564-583.

SUN, Q., WU, Y., XU, Y., CHEN, L., JANG, T. U., 2020, "Coupling Quasi-TwoDimensional Friction Model and Discrete Vapor Cavity Model for Simulation of Transient Cavitating Flows in Pipeline Systems", Mathematical Problems in Engineering.

TORO, E. F., 2009, Riemann Solvers and Numerical Methods for Fluid Dynamics. 3 ed. Berlin, Springer.

VARGAS, B. S., LISSNER, L, A., METH, S., 2017, "Características Físico-Químicas do Biodisel Conforme Especificações da Agência Nacional de Petróleo, Gás Natural e Biocombustíveis", Revista da Mostra de Trabalhos de Conclusão de Curso, v. 1, n.1, pp. 2595-3605.

WYLIE, E. B., STREETER, V. L., 1978, Fluid Transients. 2 ed. United States of America, McGraw-Hill.

ZHOU, L., WANG, H., LIU, D., MA, J., WANG, P., XIA, L., 2017, "A Second Order Finite Volume Method for Pipe Flow with Water Column Separation", Journal of Hydroenvironment Research, v. 17, pp. 47-55

8. RESPONSIBILITY NOTICE

The authors are the only responsible for the printed material included in this paper.